OCEANOGRAPHY

# Viral shunt in tropical oligotrophic ocean

**Fuh-Kwo Shiah[1,2,3], Chao-Chen Lai[1]†, Tzong-Yueh Chen[3], Chia-Ying Ko[4,5], Jen-Hua Tai[1], Chun-Wei Chang[4]***



**Viruses cause massive bacterial mortality and thus modulate bacteria-governed carbon transfer and nutrient recycling at global scale. The viral shunt hypothesis states the crucial role of viral lysis in retaining microbial carbon into food web processes, while its applicability to nature has not been well identified for over two decades. Here, we conducted nine diel surveys in the tropical South China Sea and suggested that the time scale adopted in sampling and system trophic status determine the "visibility" of the viral shunt in the field. Specifically, viral abundance (VA), bacterial biomass (BB), and bacterial specific growth rate (SGR) varied synchronously and presented the significant VA-BB and VA-SGR linkages at an hourly scale, which reveals direct interactions between viruses and their hosts. The differential responses of the viral shunt to temperature, i.e., looser VA-SGR coupling in warm and tighter VA-SGR coupling in cold environments, imply an altered carbon cycling in tropical oceans under climatic warming.**

## INTRODUCTION

Viruses and heterotrophic bacteria are the most abundant biological entities and organisms on Earth, respectively. These microbes are found on us, within us, and around us. They inhabit virtually every environment on the planet. For the general public, some of them are well known as "germs," which have played a major role in shaping society. However, only a small part of them are pathogens, and the vast majority of microbes are harmless to us.

The most significant effect of these nonpathogenic microbes on Earth is their ability to recycle the primary elements that make up all living systems (Fig. 1). Take carbon as an example, the ocean has an inventory of dissolved organic carbon (DOC) (~660 gigaton of C) roughly equal to that of atmospheric $CO_2$ (*1*, *2*). Most oceanic DOC is derived from autochthonous food web processes, e.g., algal exudation, metazoan excretion, bacteriovory, and viral lysis (*3*). Heterotrophic bacteria are the key microorganisms responsible for DOC decomposition and constitute a critical component in the "microbial loop" (*4*–*7*), which emphasizes the connections between DOC, bacteria, protozoans, and the traditional grazing (phytoplankton to zooplankton to fishes) food chain (*2*).

Viruses in aquatic environments can reduce bacteria abundance by lytic/lysogenic processes [(*8*) and citations therein]. It has been generally thought that viruses are responsible for c.a. 10 to 50% of the total bacterial mortality in surface seawater (*7*, *9*). The study of Lara *et al.* (*10*) suggested that lytic and lysogenic viruses together could release 145 gigaton of C per year in the global tropical and subtropical oceans. It has been suggested that viral lysis might affect organic carbon dynamics within the microbial loop. The viral shunt/short-circuit (*11*) or the semiclosed trophic loop (*7*) hypothesis suggested that the viral lysis process lessened the transfer of bacterial cells to protozoans and that the lysate released from the broken cells stimulated the growth of the existing bacteria. This viral shunt hypothesis undoubtedly has instated a profound influence on our knowledge of microbial biogeochemistry, but its development has based on the results of laboratory experiments and modeling only (*7*, *11*, *12*) and that its applicability to the real world has not been well documented over the past two decades [(*13*) and citations therein].

The key feature of the viral shunt hypothesis is that the viral lysis process results in a reduction of bacteria abundance accompanied by rise in lysate releasing and bacteria growth rate or the opposite with a buildup of abundance along with a decline of growth rate (*14*). It is well known that, to discern the controlling mechanism, sampling frequency should be matched to the characteristic time scales of the targeted populations. Bacterial and viral generation times in surface seawater vary at a range of hours to weeks (*15*, *16*). Daily variation of virus-bacteria relationships has been examined (*17*) in the field, but investigation at shorter time scale (i.e., hourly) has seldom been performed.

## RESULTS

### Physical properties

Surface (c.a. 5 m depth) water temperatures ranged 24.7° to 30.2°C, signaling the warm ocean's characteristics. Annually, mixed-layer depth (MLD; fig. S1) varied from c.a. 26 to 76 m with an average of 41 ± 16 m. Deeper MLD occurred during cold northeast monsoon period (November to February of the next year) and turned shallower in warm southwest monsoon period (June to September). Within each survey, the time series of MLD basically oscillated with a rhyme of the diurnal tide. The altimetry data (fig. S2 and movie S1) indicated that there was no eddy passing through the sampling station during study periods with one exception. There, a cold eddy had passed through the Southeast Asia Time Series (SEATS) station in April 2015, and its temperature was, on average, 2.1°C lower than its interannual counterpart (i.e., cruise in April 2013; fig. S1).

### Temporal-spatial variations of chemical and biological measurements

Phytoplankton biomass (PB; <2 to 97 mgC $m^{-3}$; fig. S1B) showed significant subsurface maxima, located mostly at depths of around 50 m. In general, PB showed a diurnal pattern with an ascending trend during the day time and then decreasing from dusk to dawn.

[1]Research Center for Environmental Changes, Academia Sinica, Taipei 11529, Taiwan. [2]Institute of Oceanography, National Taiwan University, Taipei 10617, Taiwan. [3]Institute of Marine Environment and Ecology, National Taiwan Ocean University, Keelung, Taiwan. [4]Institute of Fisheries Science, National Taiwan University, Taipei 10617, Taiwan. [5]Institute of Ecology and Evolutionary Biology and Master's Program in Biodiversity, National Taiwan University, Taipei 10617, Taiwan.
*Corresponding author. Email: picachueco@gmail.com
†This author contributed to this work as the first author.

Total organic carbon (TOC) concentrations ranged from 46 to 129 μM, with higher values in the surface water and then decreasing with depth in general. Subsurface TOC maxima occasionally could be seen in some cases (fig. S1C).

Bacterial biomass (BB; 2.1 to 33.8 mgC $m^{-3}$ or 0.1 to 1.7 × $10^6$ cells $liter^{-1}$) were higher in the upper 50 m and then decreased downward (fig. S1D). Subsurface BB maxima occurred in some studies. Viral abundance (VA; fig. S1E) ranged from <1 to 22 × $10^9$ particles $liter^{-1}$ with two depth patterns in general. One showed higher surface values and then decreased with depth; the other revealed subsurface VA maxima at depths of 40 to 60 m. The depth contours of VA were quite patchy. There, stacks of high-low VA readings appeared alternatively with time intervals of c.a. 6 to 12 hours. Bacterial (per cell) specific growth rate (SGR; 0.03 to 0.95 $day^{-1}$; fig. S1F) varied >30-fold in the euphotic zone. Higher bacterial growth rates (e.g., SGR > 0.2 $day^{-1}$) usually appeared in depths of >50 m.

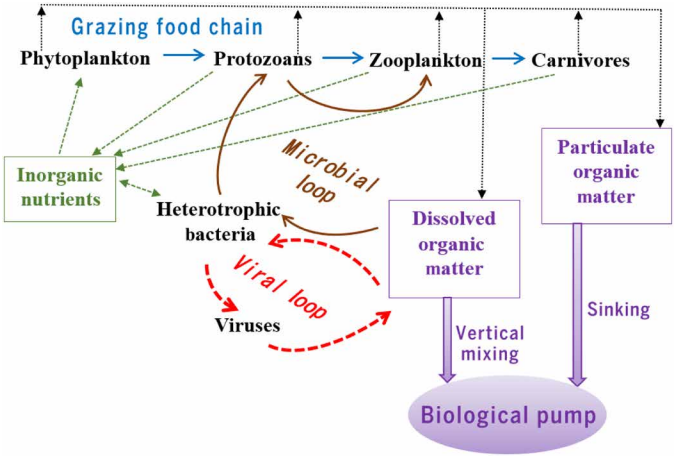


**Fig. 1. Schematic diagram of marine microbial food web.** The diagram presents key microbial processes that critically affects marine biogeochemical cycle, including the inorganic and organic fluxes (arrows) flowing among different plankton via grazing food chain (blue lines), microbial loop (brown lines), viral loop (red dashed lines), and biological pump (purple arrow).

The tempospatial pattern of the SGR readings was also quite patchy and was the opposite of VA. Neither bacterial nor viral properties showed distinct diel patterns. Bacterial production (BP), a product of BB and SGR, ranged from 0.15 to 6.97 mgC $m^{-3}$ $day^{-1}$ and was determined approximately equally by the variation of SGR and BB. The standardized partial regression coefficient ratios of SGR to BB ranged from 0.66 to 2.57 with a mean of 1.25 ± 0.64, meaning that SGR was, on average, ~25% more influential than BB in determining the variation of BP.

## Statistical relationships

Readings of BB and VA varied synchronously as a whole for the pooled data (Fig. 2A) and also individually in every cruise (Table 1). We also observed a negative BB-SGR relationship for the pooled data, and further analysis indicated that in seven of the nine cruises, distribution patterns of BB were the opposite of SGR (Table 1). For the surveys (cruises #7 and #8; Table 1) that showed no BB-SGR correlation, their contour plots were still patchy (fig. S1, D and F). Regression analysis on the pool data suggested a significant negative VA-SGR relationship (Fig. 2B) but with low $R^2$ (coefficient of determination) value. As shown in additional analyses, VA values were negatively correlated with those of SGR in six of nine cases with higher $R^2$ values ranging from 0.15 to 0.64 (Table 1).

Discrete SGR of each cruise varied negatively with temperature due to higher SGR that usually appeared in cold mid- or deep water (slopes of temperature on SGR, from −0.042 to −0.207; $R^2$ = 0.13 to 0.54; analysis not shown; fig. S1F). Significant negative correlations were observed between SGR and TOC in 9 of 10 cruises (Table 1). Note that SGR barely showed relationships with PB, which had a strong diurnal signal. In addition, the case that showed significant SGR-PB relationships was a negative one.

## Time-delay correlation and zonal analyses

Figure 3 displayed that with one exception (see below), there was a c.a. 3 to 6 hours of time lag between the peaks of depth-averaged VA (IVA) and depth-averaged SGR (ISGR) in all cruises, suggesting a regular pattern of time lag between these two measurements. After a 6-hour time lag adjustment, discrete SGR changed positively with

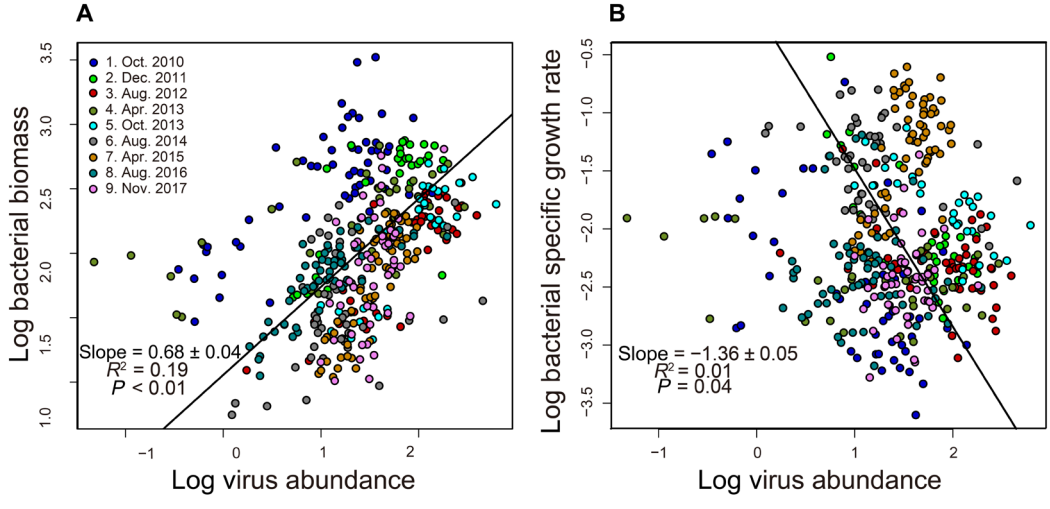


**Fig. 2. Statistical relationships between VA, BB, and bacterial SGR.** Scatterplots of (**A**) VA on BB and (**B**) VA on bacterial SGR were presented. Regression lines and summary statistics are for the pooled data.

**Table 1. The slopes and coefficients of determination ($R^2$) for the regressions among VA, BB, and bacterial SGR of the nine anchored surveys conducted at the SEATS station in the South China Sea.** Slopes were significant at $P < 0.05$ level. ns, not significant. All variables except *T* were natural log-transformed.

| Cruise # | Date | VA on BB slope ($R^2$) | BB on SGR slope ($R^2$) | VA on SGR slope ($R^2$) | Other variables* on SGR | sprc* ratio of SGR to BB |
|---|---|---|---|---|---|---|
| 1. OR1–944 | 2010.10 | +0.31(0.27) | −0.84(0.32) | −0.47(0.24) | −*T*; −TOC | 1.95 |
| 2. OR1–988 | 2011.12 | +0.68(0.55) | −0.92(0.68) | −0.85(0.65) | −*T*; −TOC | 1.38 |
| 3. OR1–1010 | 2012.08 | +0.70(0.70) | −0.52(0.32) | −0.25(0.15) | −*T*; −TOC; −PB | 0.78 |
| 4. OR1–1034 | 2013.04. | +0.23(0.36) | −0.34(0.20) | −0.12(0.16) | −*T*; −TOC | 0.85 |
| 5. OR1–1053 | 2013.10. | +0.87(0.73) | −0.64(0.79) | −0.53(0.52) | −*T*; −TOC | 0.66 |
| 6. OR1–1084 | 2014.08. | +0.36(0.18) | −0.64(0.62) | −0.24(0.15) | −*T*; −TOC | 0.87 |
| 7. OR1–1103 | 2015.04 | +1.24(0.72) | ns | +1.08(0.40) | −*T*; −TOC | 1.28 |
| 8. OR1–1144 | 2016.08 | +0.55(0.67) | ns | ns | −*T*; −TOC | 2.57 |
| 9. OR1–1184 | 2017.11 | +0.90(0.23) | −0.41(0.26) | ns | −*T* | 0.92 |

*Variables that were significantly correlated with SGR. *T*, TOC, PB, and "sprc" indicated temperature, TOC concentration, PB, and the standardized partial regression coefficient, respectively. The "sprc" measures the change in the average value of the dependent variable associated with a unit increase in the corresponding independent variable, holding constant all other independent variables.

VA (Fig. 4A). It was also true for the relationship of empirical viral turnover rate ($\lambda_{VA}$) on empirical bacterial turnover rates ($\lambda_{SGR}$), which were calculated from the change of adjacent VA and BB, respectively (Fig. 4B). The study that had been affected by the passage of cold eddy (fig. S2) had much higher SGR (0.21 to 0.33 $day^{-1}$), and there was almost no time lag between VA and SGR (Fig. 3G), suggesting alternatively a closer coupling of VA-SGR under this sporadic scenario.

The results of the cross-correlation coefficient (CCC; an index of the magnitude of harmonization of two or more time series datasets) analysis indicated a negative CCC in the treatment with no lag adjustment. The CCC increased in the 3 hours of lag treatment and then became positive, reaching the peak of the fitting curve in the 6 hours of lag treatment (Fig. 5, A and B). After separating the data into two zones, the increasing tendency of the CCC was not significant in the upper part of the euphotic zone (Fig. 5C) than that in the lower euphotic zone (depths of >50 m; Fig. 5D).

## DISCUSSION

### Physical hydrography

The SEATS station locates in deepwater areas with a bottom depth of 3800 m (*18*) and is dominated by diurnal tides (*19*). In terms of diel variation, elevated internal solitary waves in the northern South China Sea could affect bacterial properties (*20*), but these waves are confined to shallow-water areas with bottom depths of <200 m. Potential impacts from elevated internal waves were believed to be absent or very weak in the deepwater areas (*19*) such as our study site. In the cold eddy case, the values of SGR throughout the euphotic zone were significantly elevated, and its cycle was closely coupled with that of VA (Fig. 3G). Intuitively, one might give a speculation that the cooler temperature of it might be the factor driving the abovementioned phenomenon. The actual mechanism is undoubtedly interesting and important but cannot be fully identified and discussed here since we have only one cold eddy case.

### Bottom-up and top-down control processes on bacteria

Heterotrophic bacteria feed on organic matter. In a system locates at the central part of a warm ocean with almost no allochthonous organic source, a strong bottom-up (substrate supply) control on bacterial growth is naturally expected (*21*–*23*). However, the tempo-spatial patterns of SGR (fig. S1F) were out of phase with those of PB and TOC (fig. S1, A to C), indicating that substrate supply from algae, protozoans, and zooplankton sources seemed to be irrelevant to the variation of bacterial (per cell) growth rate. It is a common knowledge that bottom-up control is important in oligotrophic environment. This leads to a sensible assumption that the variation of SGR might be controlled by the lysate supply rate mediated by viruses.

The positive VA-BB relationship (Fig. 2A) has been demonstrated as a worldwide phenomenon in surface waters and sediments (*24*). Such a close linkage implied that any change in the abundance, metabolic state, and doubling time of the prokaryotic host populations will affect the VA and vice versa (*25*). A positive VA-BB linkage occurred at a shorter (e.g., hourly) time scale, revealing direct interactions (e.g., infection/lysis) between viruses and their host (*17*, *26*). The short time scale analysis (Table 1) of the VA-BB and VA-SGR relationships delivers direct field evidence supporting the argument proposed by the abovementioned researches. After the time lag adjustment, both the IVA versus ISGR (Fig. 4A) and $\lambda_{VA}$ versus $\lambda_{SGR}$ (Fig. 4B) positive relationships were significant. These phenomena indicate that viruses, either in terms of their abundance or turnover rate, can affect both the stock and rate properties of their hosts in this oligotrophic tropical ocean.

Viral shunt in this study was different in the upper and lower part of the euphotic zone (Fig. 5). We argue that temperature and the host's physiological conditions (i.e., bacterial growth rate per se) might be the two major factors in configuring the zonal feature of our field observations. For temperature effects, an early review (*25*) indicated that viral production rates changed positively with temperature in polar and cold-temperate systems, while in warm midlatitudes and tropical systems, they showed a negative trend. Later review

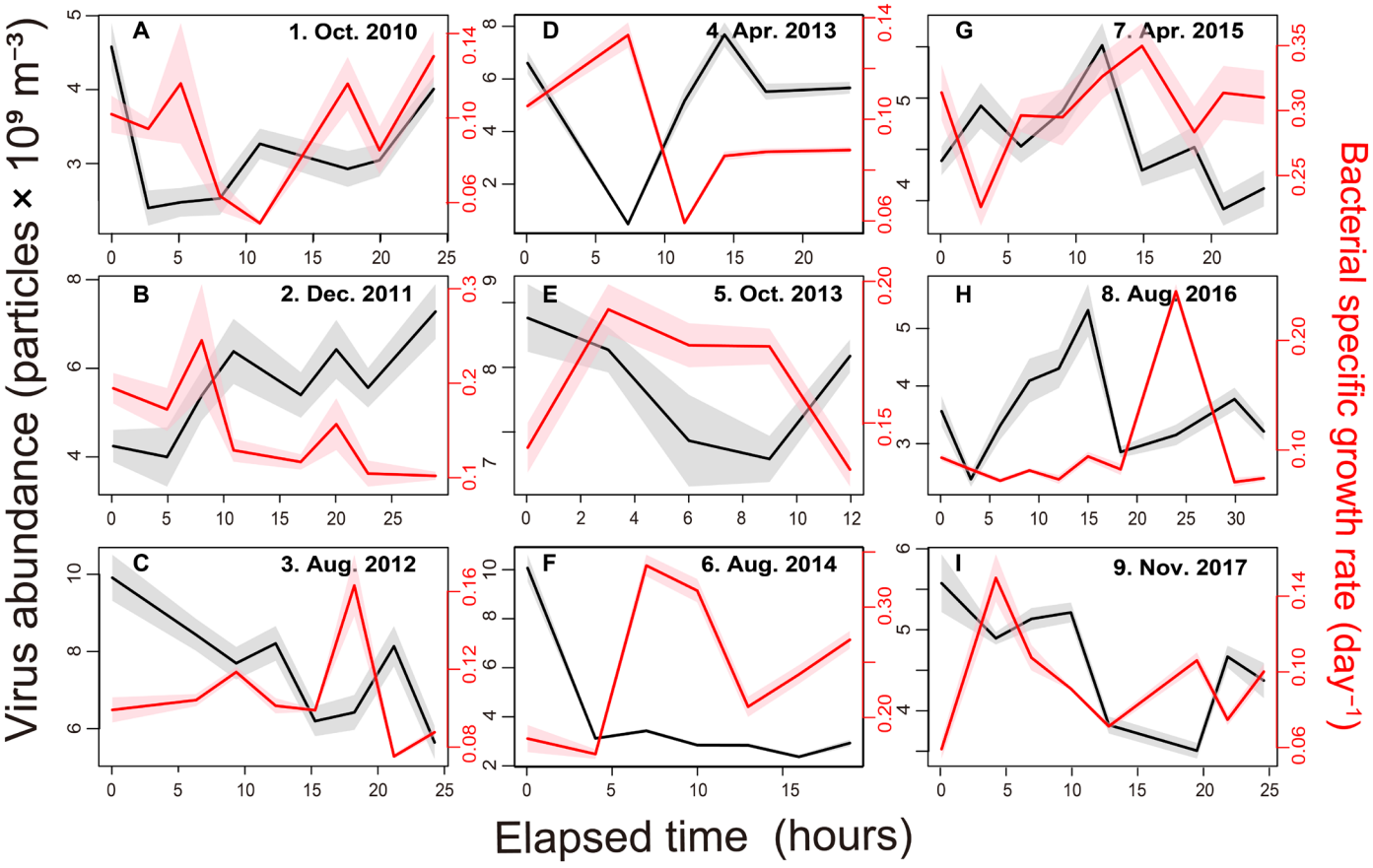


**Fig. 3. The diel changes of VA and bacterial SGRs.** All the measurements from the nine research cruises (**A** to **I**) are depth-averaged. Shaded areas indicate ±1 SEM.

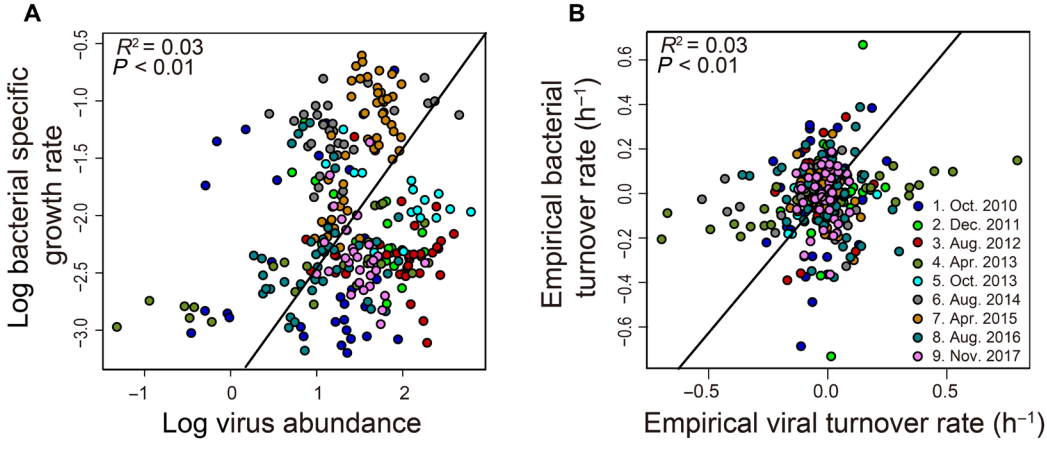


**Fig. 4. Positive effects of virus on bacterial growth at an hourly scale.** Scatterplots of the discrete (**A**) VA on bacterial SGR and (**B**) empirical viral turnover rate on empirical bacterial turnover rate were from the nine research cruises. The *X* and *Y* variables used in analysis were time delay (6 hours) adjusted.

(*27*) displayed that lysis of infected prokaryote bacteria occurred over a narrow temperature range, and the lysis processes could be inactivated at temperatures higher than the optimal temperatures (i.e., OT) ranging from 20° to 35°C.

From the perspective of the host's physiology, culture experiments (*15*) demonstrated that bacterial cell lysis rate and virus production were positive functions of SGR, meaning that inactive bacteria were less infected and or lysed. Brum *et al.* (*28*) demonstrated that, in the polar Southern Ocean, dominated temperate viruses switched from lysogeny to lytic replication as BP increased. This suggested intense seasonal changes in BP selected for temperate viruses.

In this study, higher BB (or lower SGR) values in the upper euphotic zone and lower BB (or higher SGR) readings in the lower euphotic zone (fig. S1D) roughly were separated by isotherms of 23° to 24°C

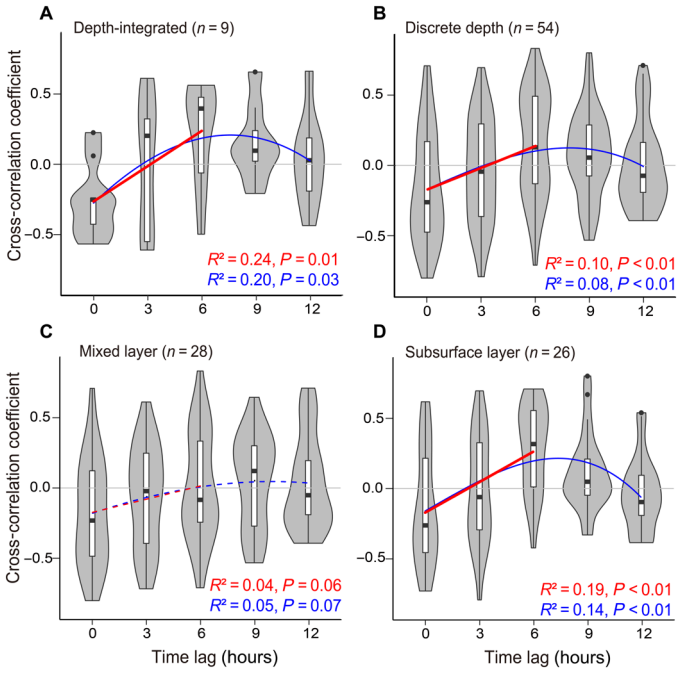


**Fig. 5. The cross-correlation analysis for the treatments of 0 to 12 hours of time lag adjustment.** Violin plots present the CCCs obtained from analyzing (**A**) IVA on ISGR, (**B**) discrete VA on discrete SGR, (**C**) IVA on ISGR in the upper part of the euphotic zone, and (**D**) IVA on ISGR in lower part of the euphotic zone. The red lines showed the tendency of increasing of the blue curve-fitting lines (0 to 6 hours). The summary statistics for these two lines are marked in red and blue, respectively.

(fig. S1A). The hypothesized mechanism asserts that the temperatures in the upper euphotic zone exceed the OT (e.g., 24°C) so that the low viral infectivity drives the accumulation of BB; as BB increases to the stationary phase, the expression of low SGR echoes substrate limitation (*21*). Even when these low SGR bacteria are infected, the long latent period might impede the lysis processes (*15*). Overall, these induce a "sluggish mode" in the upper euphotic zone, in which the rates of viral infection, bacterial growth, and lysate flux are all reduced.

On the other hand, we suggest that lower temperatures that are close to the OT in the lower euphotic zone can sustain a high viral lysis rate and result in low BB but high lysate flux. This labile substrate flux, in turn, enhances SGR when it is quickly reassimilated by existing bacteria. As mentioned above, active bacteria were more vulnerable to viral attacks than inactive ones. Moreover, these generate a "nimble mode" in the lower part of the euphotic zone. As noted by review articles (*25*, *27*), recorded inactivation temperatures for marine viruses were usually >20°C, which was higher than many virus-host systems in temperate and Arctic waters but could play a role in the tropical waters. A higher increasing tendency in the cross-correlation analysis for the lower euphotic zone (i.e., slope in Fig. 5D) implies a closer and a fast coupling between VA and SGR under a cool temperature and probably also low-light conditions.

Our study made no distinction between lytic and lysogenic viruses. The shunt and enhancing effect might be limited to, or different from, one or the other viral lifestyle (*10*, *28*). Further investigation on the succession of viral types in a similar kind of experiment can provide more insight into the context of viral shunt.

When assimilating the organic lysate for growth, inorganic nutrients are produced by bacteria due to their low growth efficiency. These regenerated inorganic nutrients could constitute a big supplement to algal production (Fig. 1), suggesting that the viral shunt could be an important link in nutrient recycling in aquatic systems (*8*, *29*). Although the following deduction may be overreaching, it is suspected that, in a warming climate, the surface layer dominated by sluggish viral shunt mode might get thicker in the tropical ocean. This infers that the supply of the inorganic nutrients derived from lysate regeneration would be lesser, while the flux of passing particulate bacteria carbon to bacterivores would be favored.

It is known that both grazing and viral lysis are density-dependent processes. The abundances of bacterivores and viruses in the oceans are in the orders of $10^5$ to $10^6$ individual liter$^{-1}$ and $10^9$ to $10^{10}$ particles liter$^{-1}$, respectively. Theoretically, viruses are much more likely to contact bacteria than bacterivores. IBB ranged from 3.4 to 19.5 mgC m$^{-3}$ in this study. Bacterial mortality was estimated by the difference between the peak and trough values during IBB's descending phase within each cycle. Calculated rates of decrease ranged from 0.11 to 1.71 mgC m$^{-3}$ hour$^{-1}$ with a mean of 0.45 ± 0.41 mgC m$^{-3}$ hour$^{-1}$ or 23 ± 20 × $10^6$ cells liter$^{-1}$ hour$^{-1}$. In the surface water of the South China Sea, the abundance of heterotrophic nanoflagellates (HNAF) and their ingestion rates ranged from 0.1 to 0.3 × $10^6$ HNAF liter$^{-1}$ and <10 to 40 cells HNAF$^{-1}$ hour$^{-1}$, respectively (*30*). Given a high HNAF abundance of 0.2 × $10^6$ HNAF liter$^{-1}$ and a high ingestion rate of 30 cells HNAF$^{-1}$ hour$^{-1}$, the HNAF engulfs ~6 × $10^6$ cells liter$^{-1}$ hour$^{-1}$, which constitutes, at most, 28% of the total mortality rate. This suggests that bacteriovory plays a less significant role than viruses in controlling BB in this system.

Marine bacteria respire on a daily basis, an amount of organic matter equivalent to about half the total marine primary production or about one-quarter of the total production of the biosphere. Bacterial activity resulting from the shunt contributes to this total. The viral shunt is an important component of the ocean (and global) carbon cycle. Correlation differs among organisms depending on the time scale that is examined, indicating that different processes operate on different scales. For field investigations conducted on time scales longer than hours, signals of virus-bacteria interactions could be blurred by other food web processes, such as bacteriovory and predations from higher trophic levels (i.e., the cascading effects) that occur in time scales of days to weeks. Despite their low abundance in the oligotrophic environments, bacteria and viruses interact within a very short (diel) time scale. This advocates that bacteria do not appear consistently under a status of starvation (famine) and that oligotrophic bacteria in the tropical ocean are "regularly" invited to a banquet (feast), depending on the potency of viral lysis. The difficulty of detecting the viral shunt in mesotrophic/eutrophic systems might be due to their abundant allochthonous and autochthonous organic input sources. It seems that there are two modes of the viral shunt in this tropical ocean. The differential temperature responses of the viral shunt modes in the upper and lower euphotic zones and the incidental cold eddy event may provide insights into viral shunt and the consequential impacts on food web processes (i.e., fueling primary production and bacteriovory) in a warming climate.

## MATERIALS AND METHODS

### Sampling

The sampling was conducted at the SEATS station (18°N, 116°E) located at the center of the northern South China Sea. Nine anchored surveys were conducted during the period of 2010–2017 (Table 1).

At the station, water samples were taken by 20 liters of Go-Flo bottles from six depths in the upper 100 m (approximately the depth of the euphotic zone) every 3 hours for at least 24 hours. Profiles of temperature, salinity, and fluorescence were recorded by sensors attached to the conductivity, temperature, and depth (CTD) rosette (General Oceanic Inc., model 1015). The MLD is defined as the depth where its temperature is 0.25°C lower than that of the surface water (*31*). Altimetry Sea Surface Height Anomalies (SSHAs) with a resolution of 0.25° were obtained from Archiving, Validation, and Interpretation of Satellite Oceanographic (AVISO) data. Those products were processed by Segment Sol Multimission Altimetry & Orbitography/Data Unification and Altimeter Combination System (SSALTO/DUCAS) and distributed by AVISO+ (www.aviso.altimetry.fr) with support from National Centre for Space Studies (CNES). The plan view of SSHAs was generated using the Generic Mapping Tools version 5 (*32*).

### Phytoplankton biomass

Chlorophyll-a was collected using the filtration (25-mm GF/F) method and was then measured with an in vitro fluorometer (Turner Designs, 10-AU-005) after acetone extraction (*33*). PB in C-unit was calculated by a conversion factor of 100 gC to 1.0 gChl-a (*34*).

### Total organic carbon

TOC is derived from the sum of particulate organic carbon (POC) and DOC. For POC, water samples (1 to 2 liters) were filtered through 200 μm of mesh to remove zooplankton and then 25-mm GF/F filters. POC concentrations were measured using a CHN analyzer (Fisons, NA1500) after samples were dried and acid-fumed. Samples for DOC were filtered through a GF/F filter. Filtrates were filled into precombusted 40-ml glass vials (Kimble). After the addition of several drops of 80% $H_3PO_4$ (Emsure, Merck), vials were sealed with precombusted aluminum foil and screw caps with Teflon-coated septa. Before analysis, samples were acidified with 2 ml of 80% $H_3PO_4$ and purged with $CO_2$-free $O_2$ at a flow rate of 350 ml $min^{-1}$ for >10 min. Samples were analyzed by the high-temperature catalytic oxidation method with a Shimadzu TOC 5000. All samples were blank-corrected (20 to 25 μM) with the deep sea water (−3000 m) from the South China Sea (DOC, 45 to 50 μM). The details of TOC measurement can be found in the previous study (*2*).

### Flow cytometry

The procedures of (*35*) and (*36*) were followed for virus/bacteria counts. Water samples were fixed with final concentrations of 1% paraformaldehyde (for viruses) and 0.1% glutaraldehyde (for bacteria) and then frozen with liquid nitrogen and stored at −80°C. Samples were stained with SYBR Green I and then incubated for 15 min at room temperature in the dark. The samples were run in a flow cytometer of CyFlow Space (PARTEC) at a rate allowing <1000 events $s^{-1}$ to avoid particle coincidence. High and low nuclear acid virus-like particles were measured but were not differentiated in abundance counting. The details of flow cytometry measurement can be found in the previous study (*2*).

### Bacterial rate parameters

Bacterial activity was determined by $^3$H-thymidine incorporation (*37*). After the injection of $^3$H-thymidine (specific activity, 20 to 85 Ci $mmol^{-1}$; final concentration, 10 nM), water samples were incubated at in situ temperature in thermos bottles for 2 hours. The water temperature in the bottles was adjusted on the basis of the temperature readings recorded from the CTD. BB and BP in C-units were derived with a thymidine and a carbon conversion factor of $1.18 \times 10^{18}$ cell $mole^{-1}$ and $20 \times 10^{-15}$ gC $cell^{-1}$, respectively (*38*). The bacterial SGR was calculated by diving production with biomass. Details of bacterial parameters can be found in (*39*).

### Data management

The depth-integrated average, an index of the bulk properties of measured variables, was derived via the trapezoidal method, and the integrated value was then divided by the deepest sampling depth. Cross-correlation analysis (*40*) tracks the movements of two or more sets of time series data relative to one another. It is used to compare multiple time series and objectively determine how well they match up with each other and, in particular, at what point the best match occurs. The possible range for the correlation coefficient of the time series data is from −1.0 to +1.0. The closer the cross-correlation value is to 1, the more closely the sets are identical. The empirical microbes turnovers rate ($\lambda_r$) calculated first the ratio of two adjacent measurements ($X_t$ and $X_{t+T}$) and then divided by the time interval ($T$) after the ratio was log-transformed. That is, $\lambda_r = \log(V_{t+T}/X_t)/T$. The $\lambda_r$ calculated from the time series data of the depth averages of VA and BB could be viewed as the analog of their turnover rates. Linear parametric analysis including multiple regression (*41*) was performed using SPSSVR software version 12.0 (IBM, Armonk, NY, USA) and R (version 4.0.3).

## SUPPLEMENTARY MATERIALS

Supplementary material for this article is available at https://science.org/doi/10.1126/sciadv.abo2829

View/request a protocol for this paper from *Bio-protocol*.

## REFERENCES AND NOTES


1. D. A. Hansell, C. A. Carlson, D. J. Repeta, R. Schlitzer, Dissolved organic matter in the ocean: A controversy stimulates new insights. *Oceanography* **22**, 202–211 (2009).
2. C.-C. Lai, C.-R. Wu, C.-Y. Chuang, J.-H. Tai, K.-Y. Lee, H.-Y. Kuo, F.-K. Shiah, Phytoplankton and bacterial responses to monsoon-driven water masses mixing in the Kuroshio off the east coast of Taiwan. *Front. Mar. Sci.* **8**, 707807 (2021).
3. M. A. Moran, E. B. Kujawinski, W. F. Schroer, S. A. Amin, N. R. Bates, E. M. Bertrand, R. Braakman, C. T. Brown, M. W. Covert, S. C. Doney, S. T. Dyhrman, A. S. Edison, A. M. Eren, N. M. Levine, L. Li, A. C. Ross, M. A. Saito, A. E. Santoro, D. Segrè, A. Shade, M. B. Sullivan, A. Vardi, Microbial metabolites in the marine carbon cycle. *Nat. Mirobiol.* **7**, 508–523 (2022).
4. L. R. Pomeroy, The ocean's food web, a changing paradigm. *Bioscience* **24**, 499–504 (1974).
5. F. Azam, T. Fenchel, J. G. Field, J. S. Gray, L. A. Meyer-Reil, F. Thingstad, The ecological role of water-column microbes in the sea. *Mar. Ecol. Prog. Ser.* **10**, 257–263 (1983).
6. F. Azam, Microbial control of oceanic carbon flux: The plot thickens. *Science* **280**, 694–696 (1998).
7. J. A. Fuhrman, Marine viruses and their biogeochemical and ecological effects. *Nature* **399**, 541–548 (1999).
8. M. Middelboe, C. P. D. Brussaard, Marine viruses: Key players in marine ecosystems. *Viruses* **9**, 302 (2017).
9. C. A. Suttle, Marine viruses—Major players in the global ecosystem. *Nat. Rev. Microbiol.* **5**, 801–812 (2007).
10. E. Lara, D. Vaqué, E. L. Sà, J. A. Bora, A. Gomes, E. Borrull, C. Díez-Vives, E. Teira, M. C. Pernice, F. C. Garcia, I. Forn, Y. M. Castillo, A. Peiró, G. Salazar, X. A. G. Morá, R. Massana, T. S. Catalá, G. M. Luna, S. Agustí, M. Estrada, J. M. Gasol, C. M. Duarte, Unveiling the role and life strategies of viruses from the surface to the dark ocean. *Sci. Adv.* **3**, e1602565 (2017).
11. S. W. Wilhelm, C. A. Suttle, Viruses and nutrient cycles in the sea: Viruses play critical roles in the structure and function of aquatic food webs. *Bioscience* **49**, 781–788 (1999).
12. J. A. Fuhrman, J. A. Cram, D. M. Needham, Marine microbial community dynamics and their ecological interpretation. *Nat. Rev. Microbiol.* **13**, 133–146 (2015).
13. M. D. Mateus, Bridging the gap between knowing and modeling viruses in marine systems—An upcoming frontier. *Front. Mar. Sci.* **3**, 284 (2017).

14. N. Y. D. Ankrah, A. L. May, J. L. Middleton, D. R. Jones, M. K. Hadden, J. R. Gooding, G. R. LeCleir, S. W. Wilhelm, S. R. Campagna, A. Buchan, Phage infection of an environmentally relevant marine bacterium alters host metabolism and lysate composition. *ISME J.* **8**, 1089–1100 (2014).
15. M. Middelboe, Bacterial growth rate and marine virus-host dynamics. *Microb. Ecol.* **40**, 114–124 (2000).
16. D. L. Kirchman, Growth rates of microbes in the oceans. *Ann. Rev. Mar. Sci.* **8**, 285–309 (2016).
17. D. M. Needham, C. E. T. Chow, J. A. Cram, R. Sachdeva, A. Parada, J. A. Fuhrman, Short-term observations of marine bacterial and viral communities: Patterns, connections and resilience. *ISME J.* **7**, 1274–1285 (2013).
18. G. T. Wong, T. L. Gu, M. Mulholland, C. M. Tseng, D. P. Wang, The South East Asian Time-series Study (SEATS) and the biogeochemistry of the South China Sea—An overview. *Deep Sea Res. II* **54**, 1434–1447 (2007).
19. A. K. Liu, Y. S. Chang, M. K. Hsu, N. K. Liang, Evolution of nonlinear internal waves in the East and South China Seas. *J. Geophys. Res.* **103**, 7995–8008 (1998).
20. T.-Y. Chen, J.-H. Ta, C.-Y. Ko, C.-h. Hsieh, C.-C. Chen, N. Jiao, H.-B. Liu, F.-K. Shiah, Nutrient pulses driven by internal solitary waves enhance heterotrophic bacterial growth in the South China Sea. *Environ. Microbiol.* **18**, 4312–4323 (2016).
21. J. J. Cole, S. Findlay, M. L. Pace, Bacterial production in fresh and saltwater ecosystems: A cross-system overview. *Mar. Ecol. Prog. Ser.* **43**, 1–10 (1988).
22. H. W. Ducklow, Factors regulating bottom-up control of bacteria biomass in open ocean plankton communities. *Arch. Hydrobiol. Beih Ergebn. Limnol.* **37**, 207–217 (1992).
23. P. Dufour, J. P. Torreton, Bottom-up and top-down control of bacterioplankton from eutrophic to oligotrophic sites in the tropical northeastern Atlantic Ocean. *Deep Sea Res. I* **43**, 1305–1320 (1996).
24. C. H. Wigington, D. Sonderegger, C. P. D. Brussaard, A. Buchan, J. F. Finke, J. A. Fuhrman, J. T. Lennon, M. Middelboe, C. A. Suttle, C. Stock, W. H. Wilson, K. E. Wommack, S. W. Wilhelm, J. S. Weitz, Re-examination of the relationship between marine virus and microbial cell abundances. *Nat. Microbiol.* **1**, 15024 (2016).
25. R. Danovaro, C. Corinaldesi, A. Dell'Anno, J. A. Fuhrman, J. J. Middelburg, R. T. Noble, C. A. Suttle, Marine viruses and global climate change. *FEMS Microbiol. Rev.* **35**, 993–1034 (2011).
26. C. Bunse, J. Pinhassi, Marine bacterioplankton seasonal succession dynamics: Review. *Trends Microbiol.* **25**, 494–505 (2017).
27. J. F. Finke, B. P. V. Hunt, C. Winter, E. C. Carmack, C. A. Suttle, Nutrients and other environmental factors influence virus abundances across oxic and hypoxic marine environments. *Viruses* **9**, 152 (2017).
28. J. R. Brum, B. L. Hurwitz, O. Schofield, H. W. Ducklow, M. B. Sullivan, Seasonal time bombs: Dominant temperate viruses affect Southern Ocean microbial dynamics. *ISME J.* **10**, 437–449 (2016).
29. E. J. Shelford, C. A. Suttle, Virus-mediated transfer of nitrogen from heterotrophic bacteria to phytoplankton. *Biogeosciences* **15**, 809–819 (2018).
30. W. H. A. Ng, H. B. Liu, Diel periodicity of grazing by heterotrophic nanoflagellates influenced by prey cell properties and intrinsic grazing rhythm. *J. Plankton Res.* **38**, 636–651 (2016).
31. S. Levitus, *Climatological Atlas of the World Ocean* (NOAA Professional Paper, 1982), p. 173.
32. P. Wessel, W. H. F. Smith, R. Scharroo, J. Luis, F. Wobbe, Generic mapping tools: Improved version released. *EOS Trans. AGU* **94**, 409–410 (2013).
33. T. R. Parsons, Y. Maita, C. M. Lalli, *A Manual of Chemical and Biological Methods for Seawater Analysis* (Pergamon Press, 1984).
34. R. W. Eppley, F. P. Chavez, R. T. Barber, Standing stocks of particulate carbon and nitrogen in the equatorial Pacific at 150°W. *J. Geophys. Res.* **97**, 655–661 (1992).
35. J. M. Gaso, P. A. D. Giorgio, Using flow cytometry for counting natural planktonic bacteria and understanding the structure of planktonic bacterial communities. *Sci. Marina* **64**, 197–224 (2000).
36. C. P. D. Brussaard, Optimization of procedures for counting viruses by flow cytometry. *Appl. Environ. Microbiol.* **70**, 1506–1513 (2004).
37. J. A. Fuhrman, F. Azam, Thymidine incorporation as a measure of heterotrophic bacterioplankton production in marine surface waters: Evaluation and field results. *Mar. Biol.* **66**, 109–120 (1982).
38. H. W. Ducklow, C. A. Carlson, Oceanic bacterial production. *Adv. Microbial Ecol.* **12**, 113–181 (1992).
39. F.-K. Shiah, G.-C. Gong, C.-C. Chen, Seasonal and spatial variation of bacterial production in the continental shelf of the East China Sea: Possible controlling mechanisms and potential roles in carbon cycling. *Deep Sea Res. II* **50**, 1295–1309 (2003).
40. R. Bracewell, Pentagram notation for cross correlation, in *The Fourier Transform and Its Applications* (McGraw-Hill, 1965), p. 243.
41. A. L. Edwards, *Multiple Regression and Analysis of Variance and Covariance* (Freeman and Company, 1985).


**Acknowledgments:** We thank the crews of R/V Ocean Researcher I and III and a dedication to late S.-C. Hsu and K.-K. Liu. **Funding:** Funding for this research came from the Taiwan MOST projects and the Ocean Acidification projects of Academia Sinica. **Author contributions:** F.-K.S., C.-W.C., and C.-C.L. conceived the research idea. C.-C.L. and T.-Y.C. performed chemical and microbial measurements. C.-W.C. and C.-Y.K. performed statistical modeling. J.-H.T. handled physical and altimetry data. F.-K.S. and C.-W.C. wrote the manuscript, with critical comments from all coauthors. **Competing interests:** The authors declare that they have no competing interests. **Data and materials availability:** All data needed to evaluate the conclusions in the paper are present in the paper and/or the Supplementary Materials. Dataset and the documentation of all analytical procedures provided as R codes are available in an online repository, at https://github.com/biozoo/ViralShunt_SEATS. The dataset needed to evaluate the conclusions and documentations of analytical procedures provided as R codes is available in the Zendo Repository, at https://doi.org/10.5281/zenodo.7017934.

Submitted 24 January 2022
Accepted 25 August 2022
Published 12 October 2022
10.1126/sciadv.abo2829